

Laser Resonators

Let us consider the reflection of a gaussian beam incident from left (complex beam parameter q_i) on a mirror of radius of curvature R . The complex beam parameter q_o of the outgoing (reflected) beam will then be given by

$$q_o = \frac{q_i A + B}{q_i C + D}. \quad (3.1)$$

The ray transfer matrix for the mirror is

$$\begin{pmatrix} A & B \\ C & D \end{pmatrix} = \begin{pmatrix} 1 & 0 \\ -2/R & 1 \end{pmatrix} \quad (3.2)$$

where R is the radius of curvature of the mirror (+ for concave and - for convex mirrors). Using this in Eq. (3.2) and $1/q = 1/R + i2/kw^2$, we find that the spot size and radius of curvature of the outgoing beam are

$$w_o = w_i \quad (3.3)$$

$$\frac{1}{R_o} = \frac{1}{R_i} - \frac{2}{R}. \quad (3.4)$$

Thus the spot size remains unchanged but, in general, the radius of curvature of the phase front changes according to Eq. (3.4). For a flat mirror ($R \rightarrow \infty$) the radius of curvature of the reflected wave also remains unchanged $R_o = R_i$. The reflected wave moving to the left is of the same type (converging or diverging) as the incident wave.

Now suppose the mirror radius of curvature R matches the radius of curvature R_i (+ for diverging and - for converging) of the incident

wavefront so that $R_i = R$ and the mirror surface coincides with the incident wavefront. Then radius of curvature of the reflected wave

$$R_o = -R_i, \quad (3.5)$$

has the same magnitude as that of the incident wavefront but opposite sign. This means the reflected wave traveling to the left will be a converging wave if the incident wave is a diverging wave and vice versa. In traveling to the left the reflected beam will retrace the path of the incident wave. If a second mirror is now placed in the path of the reflected wave traveling to the left such that the radius of curvature of the mirror matches the radius of curvature of the wavefront at the location of the second mirror, the beam will be reflected to the right retracing its path. Thus when two mirrors such that their reflecting surfaces coincide with the incident wavefronts of a gaussian beam the beam is trapped between the mirrors bouncing back and forth between the mirrors. The conditions for gaussian beam trapping are easily written down.

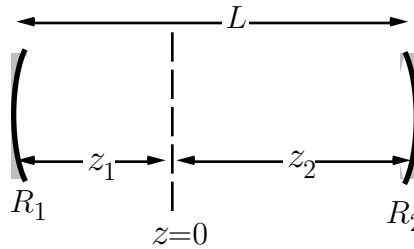


Figure 3.1: Relative to the beam waist, the mirrors in a two-mirror cavity are located at z_1 and z_2 relative to the waist in the cavity.

Suppose the mirrors with radii of curvatures R_1 and R_2 are placed at position z_1 and z_2 , respectively, relative to the beam waist [see Fig.(3.1)]. Then the trapping of a gaussian beam requires the curvature of the mirror

to match the wavefront curvature at the location of the end mirrors ¹

$$R(z_1) \equiv z_1 + \frac{z_R^2}{z_1} = -R_1, \quad (3.6a)$$

$$R(z_2) \equiv z_2 + \frac{z_R^2}{z_2} = R_2, \quad (3.6b)$$

where $z_R = \frac{1}{2}kw_0^2 = \pi nw_0^2/\lambda$ is the Rayleigh range for the beam. For a gaussian beam of minimum spot size w_0 , Eqs. (3.6a) and (3.6b) determine the radii of curvature and the positions of the mirrors relative to the waist that will trap the beam.

Often, the opposite problem, where the radii of curvatures R_1 and R_2 of the mirrors and their separation L is given and beam waist size w_0 and its location relative to M_1 (or M_2) are to be determined, is also of interest. Let us denote the locations of the mirrors M_1 and M_2 by, respectively, z_2 and z_1 relative to the beam waist. Then we have to solve Eqs. (3.6a) and (3.6b) with

$$z_2 - z_1 = L \quad (3.6c)$$

Rewriting Eqs. (3.6a)-(3.6c)

$$\frac{z_R^2}{z_1} = -(R_1 + z_1) \quad (3.7a)$$

$$\frac{z_R^2}{z_2} = R_2 - z_2 \quad (3.7b)$$

$$z_2 = z_1 + L \quad (3.7c)$$

Taking the ratio of the first two equations and eliminating z_2 from the

¹Note that these condition hold only at the end mirrors (mirrors that force the reflected beam to retrace the path of the incident beam traveling in opposite direction.)

result with the help of the last equation we obtain

$$\begin{aligned}
& \frac{z_2}{z_1} = -\frac{R_1 + z_1}{R_2 - z_2} \\
\text{or} \quad & z_2(R_2 - z_2) = -(R_1 + z_1)z_1 \\
\text{or} \quad & (z_1 + L)(R_2 - z_1 - L) = -(R_1 + z_1)z_1 \\
\text{or} \quad & z_1(R_1 + R_2 - 2L) = L^2 - R_2L \\
\text{or} \quad & z_1 = -\frac{L(R_2 - L)}{R_1 + R_2 - 2L} \tag{3.8}
\end{aligned}$$

Similarly, z_2 is given by

$$z_2 = \frac{L(R_1 - L)}{R_1 + R_2 - 2L}, \tag{3.9}$$

To calculate the waist size we substitute the expression (3.12) for z_1 in (3.9) [or Eq. (3.13) in Eq. (3.10)] and obtain

$$\begin{aligned}
z_R^2 &= -(R_1 + z_1)z_1 = \left[R_1 - \frac{L(R_2 - L)}{R_1 + R_2 - 2L} \right] \left[\frac{L(R_2 - L)}{(R_1 + R_2 - 2L)} \right] \\
&= \frac{L(R_2 - L)(R_1^2 + R_1R_2 - 2LR_1 - LR_2 + L^2)}{(R_1 + R_2 - 2L)^2} \\
&= \frac{L(R_2 - L)(R_1 - L)(R_1 + R_2 - L)}{(R_1 + R_2 - 2L)^2}
\end{aligned}$$

Using the result $z_R^2 = \pi n w_0^2 / \lambda$ we find that the waist size is given by

$$w_0 = \sqrt{\frac{\lambda}{n\pi}} \left[\frac{L(R_2 - L)(R_1 - L)(R_1 + R_2 - L)}{(R_1 + R_2 - 2L)^2} \right]^{1/4}, \tag{3.10}$$

The equations for z_1 , z_2 and w_0 can be put in more compact forms by introducing the “g-factors” defined by

$$g_i = 1 - \frac{L}{R_i}, \quad i = 1, 2. \tag{3.11}$$

Then we can write

$$R_1 = \frac{L}{1 - g_1} \quad R_2 = \frac{L}{1 - g_2}. \quad (3.12)$$

Using these in the equation for z_1 we find

$$\begin{aligned} z_1 &= -\frac{L^2(1/(1 - g_2) - 1)}{L/(1 - g_1) + L/(1 - g_2) - 2L} \\ &= -L \frac{g_2(1 - g_1)}{g_1 + g_2 - 2g_1g_2} \end{aligned}$$

Similar procedure for z_2 and w_0 can be carried out. We then obtain

$$z_1 = -\frac{g_2(1 - g_1)}{g_1 + g_2 - g_1g_2} L, \quad (3.13)$$

$$z_2 = \frac{g_1(1 - g_2)}{g_1 + g_2 - g_1g_2} L \quad (3.14)$$

$$w_0 = \sqrt{\frac{L\lambda}{n\pi}} \left[\frac{g_1g_2(1 - g_1g_2)}{(g_1 + g_2 - 2g_1g_2)^2} \right]^{1/4} \quad (3.15)$$

Using the propagation law for the spot size of a gaussian beam, we find the spot sizes at the mirrors are given by

$$w_1 = w_0 \sqrt{1 + \frac{z_1^2}{z_R^2}} = \sqrt{\frac{L\lambda}{n\pi}} \left[\frac{g_2}{g_1(1 - g_1g_2)} \right]^{1/4} \quad (3.16)$$

$$w_2 = w_0 \sqrt{1 + \frac{z_2^2}{z_R^2}} = \sqrt{\frac{L\lambda}{n\pi}} \left[\frac{g_1}{g_2(1 - g_1g_2)} \right]^{1/4} \quad (3.17)$$

An inspection of Eqs. (3.15), (3.16) and (3.17) for spot sizes shows that for physical (real and positive) beam spot sizes g_1 and g_2 must have the same sign so that the product g_1g_2 is positive and confined to the range

$$0 < g_1g_2 < 1 \quad (3.18)$$

If this condition is not satisfied stable gaussian beam solutions do not exist for the given mirror configuration. Resonators with R_1 , R_2 , and L satisfying condition (3.18), admit gaussian beam modes and are said to be stable. The condition for stability of resonators for admitting gaussian beam mode solutions coincides with the condition for trapping paraxial rays.

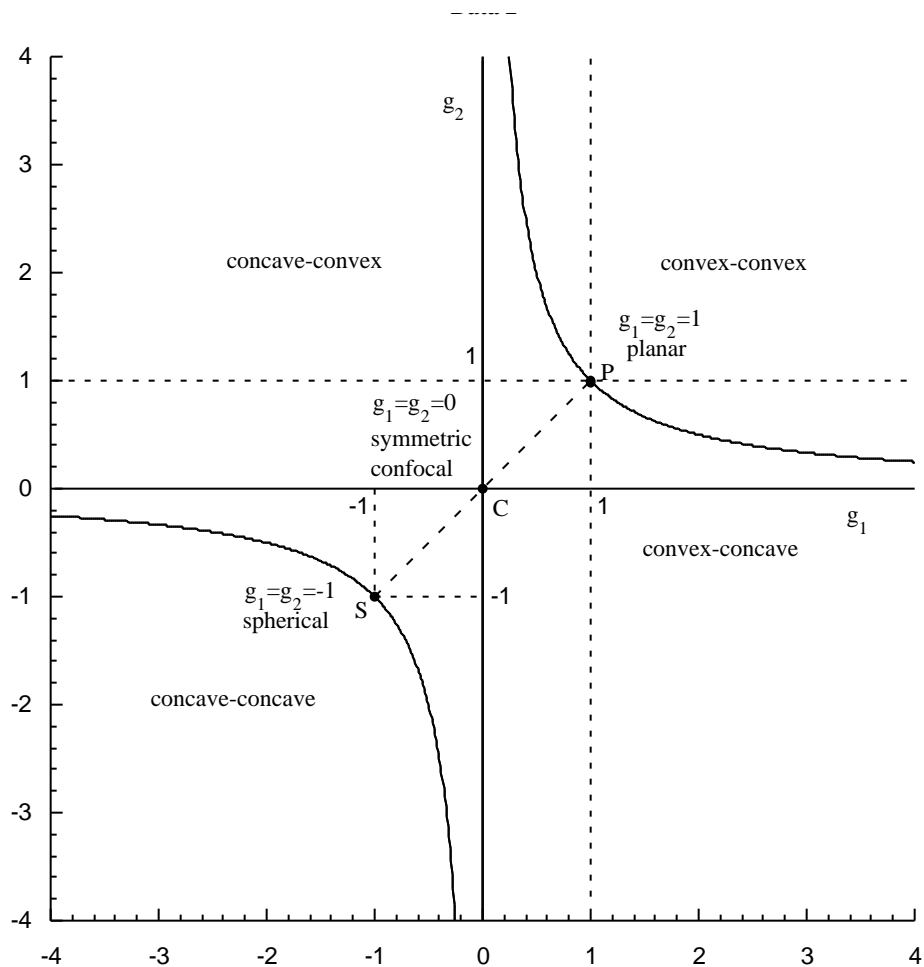


Figure 3.2: Stable two-mirror resonators lie in the region bounded by the two branches of the rectangular hyperbola $g_1g_2 = 1$ and the coordinate axes $g_1 = 0$ and $g_2 = 0$ in the $g_1 - g_2$ plane.

For cartesian symmetry, the gaussian beam modes are known as the Hermite-gaussian modes

$$\mathcal{E}_{\ell mp}(\vec{r}, t) = A \frac{w_0}{w(z)} H_\ell \left(\frac{\sqrt{2}x}{w(z)} \right) H_m \left(\frac{\sqrt{2}y}{w(z)} \right) e^{-\rho^2/w^2(z) - i\omega t} \sin[\Phi_{\ell m}(z)] \quad (3.19)$$

where

$$w(z) = w_0 \sqrt{1 + z^2/z_R^2}, \quad (3.20)$$

$$R(z) = z + z_R/z, \quad (3.21)$$

$$z_R = \pi n w_0^2 / \lambda, \quad (3.22)$$

$$\Phi_{\ell m}(z) = kz + k\rho^2/2R(z) - \psi_{\ell m}(z) + \phi_0 \quad (3.23)$$

$$\psi_{\ell m}(z) = (\ell + m + 1) \tan^{-1}(z/z_R), \quad (3.24)$$

and ϕ_0 is some phase angle to be determined by the boundary conditions. Note that instead of traveling gaussian waves we now have standing gaussian waves because the gain medium will generate gaussian beams traveling in opposite directions which will overlap to form standing waves. This imposes an additional requirement - for the field to be single valued we require that the round trip phase shift be an integer multiple of 2π or single pass phase shift $\Phi_{\ell m}(z_2) - \Phi_{\ell m}(z_1)$ be an integer multiple of π ,

$$\begin{aligned} \Phi_{\ell m}(z_2) - \Phi_{\ell m}(z_1) &\equiv k(z_2 - z_1) - (\ell + m + 1) \left(\tan^{-1} \frac{z_2}{z_R} - \tan^{-1} \frac{z_1}{z_R} \right) \\ &\quad + k\rho^2 \left(\frac{1}{R_2} + \frac{1}{R_1} \right) = p\pi \end{aligned} \quad (3.25)$$

where we have used $R(z_1) = -R_1$ and $R(z_2) = R_2$. The term involving $k\rho^2$ is negligible compared to kL as ρ is a few spot sizes in magnitude and beam spot size is small compared with both R and L ,

$$\frac{1}{kL} \left[\frac{k\rho^2(R_1 + R_2)}{R_1 R_2} \right] \approx \frac{w^2}{RL} \ll 1. \quad (3.26)$$

The \tan^{-1} terms can be combined to give

$$\tan^{-1} \frac{z_2}{z_R} - \tan^{-1} \frac{z_1}{z_R} = \tan^{-1} \frac{(z_2 - z_1)z_R}{z_R^2 + z_1 z_2} = \tan^{-1} \frac{Lz_R}{z_R^2 + z_1 z_2}. \quad (3.27)$$

Using the expressions for z_1 , z_2 , and z_R given in Eqs. (3.13)-(3.15) in this equation we obtain

$$\tan^{-1} \frac{z_2}{z_R} - \tan^{-1} \frac{z_1}{z_R} = \tan^{-1} \sqrt{\frac{1 - g_1 g_2}{g_1 g_2}} = \cos^{-1} \sqrt{g_1 g_2} \quad (3.28)$$

Using the results of Eqs. (3.26) and (3.28) in Eq. (3.25) the mode condition becomes

$$kL - (\ell + m + 1) \cos^{-1} \sqrt{g_1 g_2} = p\pi \quad (3.29)$$

This equation determines k which now depends on three indices

$$k_{\ell mp} = \frac{\pi}{L} \left[p + (\ell + m + 1) \frac{\cos^{-1} \sqrt{g_1 g_2}}{\pi} \right]. \quad (3.30)$$

From the relation $k_{\ell mp} = n2\pi\nu_{\ell mp}/c$ we find the resonator eigen-frequencies are given by

$$\nu_{\ell mp} = \frac{c}{2nL} \left[p + (\ell + m + 1) \frac{\cos^{-1} \sqrt{g_1 g_2}}{\pi} \right] \quad (3.31)$$

From this we see that each axial mode frequency ν_{00p} has a number of transverse mode (indices ℓmp with p fixed) frequencies associated with it. Consecutive axial and transverse modes are separated, respectively, by

$$\Delta\nu_{ax} \equiv \nu_{00p+1} - \nu_{00p} = \frac{c}{2nL}, \quad (3.32)$$

$$\Delta\nu_{tr} \equiv \nu_{(\ell+1)mp} - \nu_{\ell mp} = \nu_{\ell(m+1)p} - \nu_{\ell mp} = \frac{c}{2nL} \left[\frac{\cos^{-1} \sqrt{g_1 g_2}}{\pi} \right]. \quad (3.33)$$

Resonator mode functions can then be written as ($\omega_{\ell mp} = 2\pi\nu_{\ell mp}$)

$$E_{\ell mp} = \mathcal{A} \frac{w_0}{w(z)} H_\ell \left(\frac{\sqrt{2}x}{w(z)} \right) H_m \left(\frac{\sqrt{2}y}{w(z)} \right) e^{-\frac{\rho^2}{w^2(z)} - i\omega_{\ell mp} t} \sin[\Phi_{\ell mp}(z)], \quad (3.34)$$

where

$$\Phi_{\ell mp}(z) = [k_{\ell mp}z - (\ell + m + 1)\psi_{\ell m}(z) + k\rho^2/2R(z)] \quad (3.35)$$

3.0.1 Symmetric Resonators

An important class of stable resonators are the symmetric resonators for which $R_1 = R_2 \equiv R$ and $-z_1 = z_2 = L/2$ so that $g_1 = g_2 \equiv g = 1 - L/R$. These resonators lie along the line $g_1 = g_2$ in the $g_1 - g_2$ plane [see Fig(3.2)]. By symmetry the beam waist occurs at the center of the resonator $z = 0$ and the minimum spot size there is given by

$$w_0 = \sqrt{\frac{L\lambda}{2n\pi}} \left[\frac{1+g}{1-g} \right]^{1/4} = \sqrt{\frac{\lambda}{2n\pi}} [L(2R-L)]^{1/4}. \quad (3.36)$$

Spot sizes at the two mirrors are equal and given by

$$w_1 = w_2 = \sqrt{\frac{L\lambda}{n\pi}} \left[\frac{1}{1-g^2} \right]^{1/4} = \sqrt{\frac{\lambda}{n\pi}} \left[\frac{LR^2}{2R-L} \right]^{1/4}. \quad (3.37)$$

We will discuss three special cases of symmetric stable resonators.

Long Radius Near Planar Resonators

These resonators are characterized by $R_1 \approx R_2 \equiv R \gg L$ so that $g_1 \approx g_2 = 1 - L/R \approx 1$. Then beam spot sizes are

$$w_0 = \sqrt{\frac{\lambda}{n\pi}} \left[\frac{RL}{2} \right]^{1/4} (1 - L/2R)^{1/4} \approx \sqrt{\frac{\lambda}{n\pi}} \left[\frac{RL}{2} \right]^{1/4}, \quad (3.38)$$

$$w_1 \approx w_2 = \sqrt{\frac{\lambda}{n\pi}} \left[\frac{RL}{2} \right]^{1/4} \frac{1}{(1 - L/2R)^{1/4}} \approx w_0 \left[1 - \frac{L}{4R} \right] \quad (3.39)$$

Hence in near planar resonators beam waist is large and varies little over the length of the resonator ($w_1 = w_2 \approx w_0$). This is a useful feature

for extracting energy more efficiently from the gain medium in a laser. Large spot size means that laser beams produce by such cavities will have low divergence. These advantages are accompanied by the difficulty in maintaining the alignment of mirrors. Since these resonators are close to instability region, small perturbations in mirror orientation can easily misalign resonator axis. Mirrors with large radius of curvature are difficult to manufacture. For example a $D = 2.50$ cm diameter mirror with $R = 20$ m has a sag at the center of only $D^2/8R \approx 4 \mu\text{m}$. Nevertheless resonators utilizing mirrors with radius of curvature $R \sim 10$ m are commonly used in gas lasers.

Frequency spectrum of these resonators can also be discussed. Since $g_1 = g_2 = 1 - L/R \approx 1$ the angle $\psi = \cos^{-1} \sqrt{g_1 g_2} = \cos^{-1}(1 - L/R)$ is a small angle close to zero. Using the small angle approximation $\cos \psi \approx 1 - \psi^2/2$ we find $\cos \psi \approx 1 - \psi^2/2 = \sqrt{g_1 g_2} = (1 - L/R)$ so that the angle ψ is given by

$$\psi = \sqrt{2L/R}.$$

Then the mode frequency spectrum for near planar resonators becomes

$$\nu_{\ell mp} = \frac{c}{2nL} \left[p + \frac{(\ell + m + 1)}{\pi} \sqrt{2L/R} \right] \quad (3.40)$$

The axial and transverse mode separations are given by

$$\Delta\nu_{ax} = \frac{c}{2nL} \quad (3.41)$$

$$\Delta\nu_{tr} = \frac{c}{2nL} \left[\frac{1}{\pi} \sqrt{\frac{2L}{R}} \right] \ll \Delta\nu_{ax} \quad (3.42)$$

Hence piled up on the high frequency side of each axial mode is a cluster of transverse modes as shown in Fig. (3.3). Note that for a fixed value of axial index p , all transverse modes with $\ell + m = \text{const}$ are degenerate. For example, modes $01p$ and $10p$ are degenerate. Similarly $02p$, $11p$ and $20p$ are degenerate.

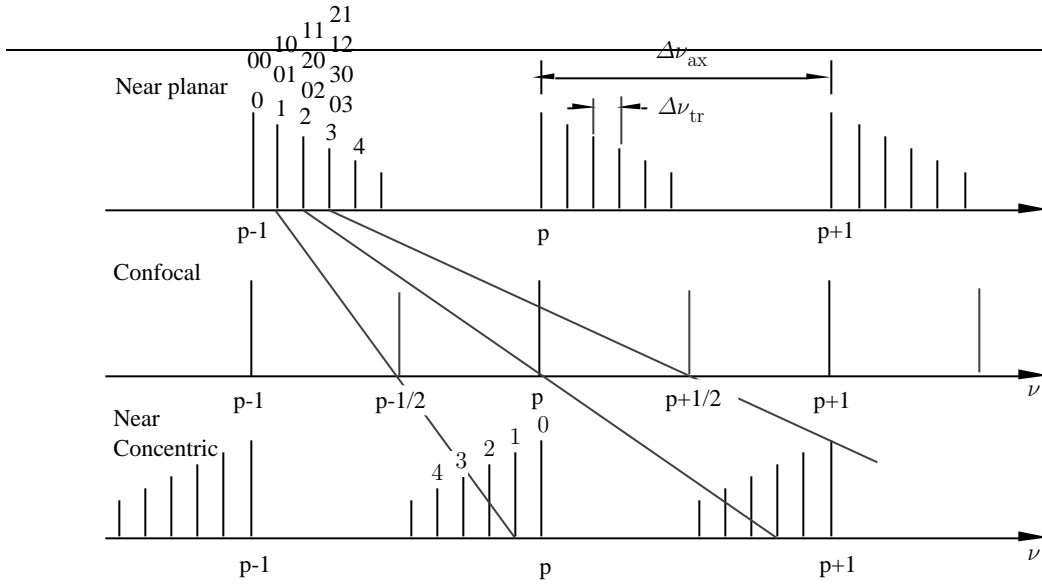


Figure 3.3: Frequency spectrum of symmetric two-mirror resonators with Hermite-Gauss modes. The dashed lines show the trajectories of mode frequencies as the resonator evolves from plane parallel to a concentric resonator.

Symmetric Confocal Resonator

Another important symmetric resonator that lies, literally, at the heart of stable resonators is the symmetric confocal resonator. This resonator is characterized by $g_1 = 0 = g_2$ (point C) corresponding to $R_1 = R_2 \equiv R = L$. Since for a concave spherical mirror the focal point lies a distance $R/2$ in front of it, it is clear that for $L = R$ the focal points of the two mirrors coincide. Hence the name confocal. Note that there are other confocal resonators indicated by the dashed curve $L = \frac{1}{2}(R_1 + R_2)$. All confocal resonators except the symmetric resonator are unstable.

For the symmetric confocal resonator the beam waist lies at the center of the resonator. Spot sizes at the waist and mirrors are given by

$$w_0 = \sqrt{\frac{L\lambda}{2n\pi}}, \quad (3.43)$$

$$w_1 = \sqrt{\frac{L\lambda}{n\pi}} = \sqrt{2}w_0. \quad (3.44)$$

Thus in propagating from the beam waist to an end mirror the spot radius increases by $\sqrt{2}$. Hence in the confocal resonator mirror separation is exactly equal to the confocal parameter of the beam. On the average (averaged over the entire resonator) the confocal resonator has the smallest spot size of all stable resonator. This feature is useful if high power density is desired over the entire resonator length. Small mode volume associated with small beam size, however, may not be the most efficient for energy extraction in a laser if the gain volume does not match the mode volume. Small mode volume of the fundamental mode may encourage transverse modes to oscillate and this may degrade the spatial profile of the beam. Matching gain profile to mode volume is a fundamental consideration in the design of laser resonators.

This resonator is insensitive to small perturbations of mirror position and orientation because any tilt of either mirror still leaves the center of curvature located at the other mirror. This merely displaces the resonator axis by a small amount. This insensitivity combined with high degree of degeneracy of mode spectrum makes symmetric confocal resonators ideal for scanning spectrum analyzer applications.

Frequency spectrum of the confocal resonator has high degree of degeneracy. Since $g = 0$ it follows that $\psi = \cos^{-1}(0) = \pi/2$ and the mode spectrum becomes

$$\nu_{lmp} = \frac{c}{4nL}(2p + m + p + 1). \quad (3.45)$$

This spectrum gives axial and transverse modes separated by

$$\Delta\nu_{ax} = \frac{c}{2nL}, \quad (3.46)$$

$$\Delta\nu_{tr} = \frac{c}{4nL}. \quad (3.47)$$

Thus the spectrum has a simple structure and successive modes in a con-

focal (axial or transverse) are separated by

$$\Delta\nu_C = \frac{c}{4nL}.$$

There is high degree of degeneracy. For example, modes $00p$, $20(p-1)$, $11(p-1)$, $01(p-1)$, $40(p-2)$, $31(p-2)$, $22(p-2)$, $13(p-2)$, $04(p-2)$, etc are degenerate.

Concentric or spherical resonators

These resonators lie near the boundary of the stability region in the third quadrant of the $g_1 - g_2$ plane. They are characterized by $L \approx 2R$. Writing $L = 2R(1 - \delta)$ where $0 < \delta \ll L, R$ we obtain

$$g_1 = g_2 = 1 - \frac{L}{R} = 1 - \frac{2(R - \delta)}{R} = -1 + \frac{2\delta}{R} \quad (3.48)$$

Using this we obtain for the beam spot sizes

$$w_0 = \sqrt{\frac{L\lambda}{2\pi n}} \left[\frac{1+g}{1-g} \right]^{1/4} \approx \sqrt{\frac{L\lambda}{2\pi n}} \left[\frac{2\delta/R}{2} \right]^{1/4} = \sqrt{\frac{L\lambda}{2\pi n}} \left[\frac{\delta}{R} \right]^{1/4} \quad (3.49)$$

$$w_1 = \sqrt{\frac{L\lambda}{\pi n}} \left[\frac{1}{1-g^2} \right]^{1/4} \approx \sqrt{\frac{L\lambda}{\pi n}} \left[\frac{1}{2 \times (2\delta/R)} \right]^{1/4} = \sqrt{\frac{L\lambda}{2\pi n}} \left[\frac{R}{\delta} \right]^{1/4} \quad (3.50)$$

In this case the minimum spot size w_0 at the center of the resonator becomes very small whereas the spot size at the mirrors $z_2 = -z_1 \approx R$ becomes very large $w_1 = w_2 \gg w_0$. The central spot has very high power density and may be useful in some nonlinear optical applications but from the point of view of energy extraction from the gain medium in a laser this is not very useful. The beam divergence is also very large. Spherical resonators are also very sensitive to small mirror misalignments which can produce large changes in the resonator axis. res

Frequency spectrum of a spherical resonator is also easily calculated. From Eq.(3.48) we note $g_1 = g_2 = -1 + 2\delta/R \approx -1$. The angle $\psi = \cos^{-1} \sqrt{g_1 g_2} = \cos^{-1} [-1 + 2\delta/R] \approx \cos^{-1}(-1)$ is close to π . Writing this angle as $\psi = \pi - \phi$ we obtain

$$\cos(\pi - \phi) = -\cos\phi \approx -\left(1 - \frac{\phi^2}{2}\right) = \left[-1 + \frac{2\delta}{R}\right] \quad (3.51)$$

This gives $\phi \approx 2\sqrt{\delta/R}$ and $\Psi = \pi - 2\sqrt{\delta R}$. The spectrum for a spherical resonator can then be written

$$\begin{aligned} \nu_{\ell mp} &= \frac{c}{2nL} \left(p + \frac{(\ell + m + 1)}{\pi} \left(\pi - 2\sqrt{\frac{\delta}{R}} \right) \right) \\ &= \frac{c}{2nL} \left(p + \ell + m + 1 - (\ell + m + 1) \frac{2}{\pi} \sqrt{\frac{\delta}{R}} \right) \end{aligned} \quad (3.52)$$

Mode frequency separation is then given

$$\Delta\nu_{ax} = \frac{c}{2nL}, \quad (3.53)$$

$$\Delta\nu_{trans} = \frac{c}{2nL} \left(1 - \frac{2}{\pi} \sqrt{\frac{\delta}{R}} \right) = \Delta\nu_{ax} \left(1 - \frac{2}{\pi} \sqrt{\frac{\delta}{R}} \right) \quad (3.54)$$

Thus the transverse mode spacing is only a little less than the axial mode separation. This means the modes $\nu_{01p} = \nu_{10p}$ approach $\nu_{00(p+1)}$ from the low frequency side, modes $\nu_{02p} = \nu_{11p} = \nu_{02p}$ approach $\nu_{00(p+2)}$ from the low frequency side. Thus each axial mode carries a pile of mode on its low frequency side. The trajectories of various transverse modes as a resonator changes from a near-planar through confocal to near-spherical is shown in Fig. (3.3).